JOURNAL OF CATALYSIS **164,** 152–165 (1996)
ARTICLE NO. 0371

Electronic and Chemical Properties of the $Pt_{80}Fe_{20}(111)$ Alloy Surface: A Theoretical Study of the Adsorption of Atomic H, CO, and Unsaturated Molecules

F. Delbecq and P. Sautet

Institut de Rercherches sur la Catalyse, CNRS, 2 Avenue Albert Einstein, 69626 Villeurbanne Cedex, France; and Ecole Normale Supérieure de Lyon, 46 Allée d'Italie, 69364 Lyon Cedex 07, France

Received December 14, 1995; revised May 25, 1996; accepted July 29, 1996

By means of semiempirical extended Hückel calculations, the electronic properties of the surface Pt atoms in the $Pt_{80}Fe_{20}(111)$ alloy have been compared with those of pure Pt(111). Two types of surface Pt atoms exist, depending on the presence or not of a Fe atom as first neighbor in the second layer. An electron transfer occurs from Fe to Pt resulting in an increased electron density on the surface Pt atoms. The transfer is larger for Pt atoms having no Fe as neighbor. All adsorbed molecules have smaller binding energies on the alloy than on pure Pt. This is essentially due to an increase of the repulsions resulting from the increased electron density. An important result is that the adsorption sites and the geometries of the adsorbates are not the same on the alloy and on pure Pt, which explains the modifications in the catalytic properties of Pt when it is alloyed with Fe.

I. INTRODUCTION

It is well known that alloying two metals modifies their physical and chemical characteristics and especially can improve their catalytic properties. For example, the hydrogenation rate of cinnamaldehyde and the selectivity to unsaturated alcohol is strongly enhanced when Pt is alloyed with Fe (1). This alloying effect has been investigated on a model catalyst, the (111) face of the single crystal $Pt_{80}Fe_{20}$ alloy, in the hydrogenation of α–β unsaturated aldehydes (2) and of butadiene (3). The reactivity is enhanced (TOF is multiplied by 3–5) and the selectivity is increased by 25–30%. This surface has been well characterized by LEED (4) and X-ray photoemission core level spectroscopy (5). The first layer is nearly pure Pt and the layers below have a bulk-like structure with the fcc Pt_3Fe ordered arrangement. This Pt_3Fe structure corresponds to a $Pt_{75}Fe_{25}$ composition and therefore, in the real $Pt_{80}Fe_{20}$ structure, some of the Fe atoms are randomly replaced by Pt atoms to obtain the correct stoichiometry. This effect will be neglected in this study where a Pt_3Fe bulk structure will be considered. In that model case, excluding the entirely Pt surface layer, all layers have the Pt_3Fe composition with a (2×2) ordered Fe lattice in the (111) Pt plane. This alloy is of fundamental interest because it does not expose different metals at the (111) surface, but only Pt atoms like a simple Pt(111) surface. However, these surface Pt atoms are not equivalent since they have different first neighbor atoms in the second layer. One-quarter of the surface Pt atoms are bonded to three Pt atoms in the sublayer and three-quarters have two Pt and one Fe atoms as neighbors in the sublayer. The results of the adsorption of CO and H on this surface confirm the existence of the two kinds of Pt atoms (6, 7).

Our aim in this work is to study the electronic properties of the $Pt_{80}Fe_{20}(111)$ surface alloy modeled by $Pt_{75}Fe_{25}$ by means of theoretical calculations in order to explain its behavior toward adsorption and catalytic reactions. This means that we wish to understand how different are the chemisorptive properties of the two types of surface Pt atoms, comparing those with 9 Pt as neighbors with those with 1 Fe and 8 Pt as neighbors. This system is indeed an excellent example by which to address the problem of the electronic effects in transition metal alloys and of their influence on adsorption properties.

The methods used are based on the extended Hückel theory which allows one to investigate the adsorption of large organic molecules. First we will compare the electron distribution and the shape of the orbitals for the surface Pt atoms of the alloy with those of the pure Pt(111) surface. Then we will adsorb H, CO, ethylene, formaldehyde, and acrolein on both surfaces and compare the results in relation with the catalytic properties.

II. METHODOLOGY

Our calculations are of the tight binding extended Hückel type. Two kinds of method have been used. The first is based on the Bloch theorem and deals with the properties of a periodic surface. It allows the study of bare surfaces and of small adsorbed molecules such as H or CO. For larger molecules this method is less convenient since large surface unit cells must be chosen in order to avoid interactions

0021-9517/96 $18.00

between the adsorbates. In these cases, we prefer the molecular method already used by us to study the adsorption of alkenes or aldehydes on surfaces (8). In this method the surface is modeled by a large cluster divided into a core part and an outer shell in order to correct the edge effects. With both methods (using slab or cluster), most of the interpretations are based on the density of states (DOS) curves.

The choice of the electronic parameters (atomic orbital energies and exponents) is crucial for studying a bimetallic system since they must take into account the relative properties of the two metals. For platinum we have kept the parameters used in our previous work and we have adjusted the orbital energies of iron. Two experimental results have guided us in this choice. First, it has been determined that the work function is lowered by 0.2 eV for the clean alloy surface compared to pure Pt (7). Second, it is known from EXAFS measurements that there is an electron transfer from Fe to the Pt *d* band of about 0.1 electron (9). Hence we have varied the values of the orbital energies (H_{ii}'s) given by Saillard and Hoffmann for metallic iron without changing the exponents (10). An energy of −10.5 eV for the Fe *d* orbitals leads to a variation of 0.22 eV in the Fermi level and an increase of 0.13 e^- in the *d*-band population of the surface Pt atoms. This is the selected value throughout this work. A value of −9.9 eV is used in some cases for the interpretations since it allows us to amplify the electronic population variations caused by alloying. The parameters of C, H, O for the adsorbed molecules are the same as those in our previous works. All these parameters are gathered in Table 1.

For the periodic calculations a three-layer slab has been used. The unit cell contains 12 atoms, four Pt in the first layer and three Pt plus one Fe in the other layers (see Fig. 1). For cluster calculations, the principle that we use for building

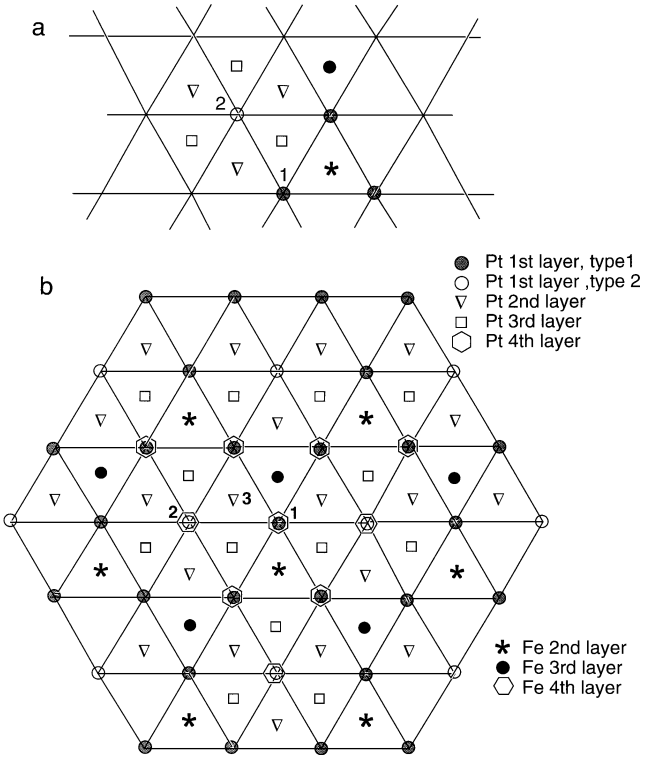

FIG. 1. Position of the various atoms (a) in the three layer slab and (b) in the $Pt_{77}Fe_{15}$ cluster.

the cluster is to place in the core all atoms involved in the adsorption and their first neighbors. The (111) surface of the Pt_3Fe alloy presents several types of bridge and hollow sites. In order to describe all adsorption sites similarly, a cluster of C_{3V} symmetry must be considered. This leads us to build a cluster of 92 atoms with a core of 37 atoms to represent the (111) face of pure Pt. For the alloy, 15 Pt atoms have been replaced by Fe atoms leading to the cluster called $Pt_{77}Fe_{15}$ (core $Pt_{33}Fe_4$) which is shown in Fig. 1. The metal–metal distance has been kept at 2.77 Å as in pure Pt since the lattice parameter of the alloy is only 0.02 Å shorter than that of the pure metal.

In the following, we will study first the electronic structure of the alloy surface and then the adsorption of several molecules of interest in catalysis.

TABLE 1

Parameters for the Extended Hückel Calculations

Atom	Orbital	H_{ii} (eV)	$\zeta_1{}^a$	$\zeta_2{}^a$	$C_1{}^b$	$C_2{}^b$
Pt	6*s*	−9.29	2.544			
	6*p*	−4.48	2.544			
	5*d*	−11.26	6.013	2.696	0.6333	0.5512
Fe	4*s*	−8.9	1.9			
	4*p*	−5.1	1.9			
	3*d*	−10.5	5.35	1.8	0.5366	0.6678
C	2*s*	−19.7	1.625			
	2*p*	−9.7	1.625			
O	2*s*	−30.6	2.275			
	2*p*	−13.1	2.275			
H	1*s*	−12.1				

[a] Slater exponents.
[b] Coefficients in double ζ expansion.

III. STRUCTURE OF THE $Pt_{80}Fe_{20}(111)$ SURFACE

As mentioned in the Introduction and as can be observed in Fig. 1, there are two types of Pt surface atoms. A Pt atom of type 1, called Pt(1), has two Pt and one Fe as first neighbors in the second layer while a Pt atom of type 2, called Pt(2), has three Pt as first neighbors. As stated above in regard to the determination of the Fe parameters, there is an electron transfer from Fe to Pt in the alloy. However, the transfer is different for the two types of Pt atoms on the

surface. For Pt of type 1 it is globally 0.16 e^- and 0.13 e^- in the *d* band. It is slightly larger for Pt of type 2 with overall 0.24 e^- and 0.21 e^- in the *d* band. They both gain 0.02 e^- in the *s* band and 0.01 e^- in the *p* band. Therefore the surface Pt atoms which are the most modified by alloying are those of type 2, which are surprisingly the ones not in contact with a Fe atom.

If one analyzes more precisely what happens for each orbital, one notices that the orbitals whose population changes the most are $d_{x^2-y^2}$, d_{xy}, and *s*. The other orbitals, d_{z^2}, d_{xz}, and d_{yz}, vary little. Figure 2 presents the DOS projected on the orbitals of a type 1 Pt atom of the surface alloy compared with a pure Pt surface. The shape of the DOS projected on d_{xy} and $d_{x^2-y^2}$ does not change much when Pt is alloyed with Fe. Effectively these two orbitals have their electron density mostly in the surface plane and therefore are weakly affected by the Fe atom which lies in the second layer. However, the Fermi level is shifted up in the alloy which results in a larger part of the $d_{x^2-y^2}$ or d_{xy} band lying below this level and hence in more populated orbitals. In contrast, the d_{z^2}, d_{xz}, and d_{yz} orbitals, which have a good overlap with metal atoms of the second layer, are strongly involved in the interaction with the Fe orbitals. For example, the overlap population between d_{xz} Pt(1) and d_{xz} Fe is $+0.53 \times 10^{-2}$ in $Pt_{80}Fe_{20}$ compared to -0.59×10^{-3} in pure Pt (Fe replaced by Pt). The *d*–*d* interaction, which was repulsive in Pt, becomes attractive in $Pt_{80}Fe_{20}$. This is illustrated by the crystal orbital overlap population (COOP) curves of Figs. 3a and 3b which show the overlap population curve between d_{xz} Pt(1) and the d_{xz} orbital of the nearest Fe atom in the second layer (Fig. 3b) and the overlap population curve between d_{xz} Pt(1) and the d_{xz} orbital of the Pt atom which occupies the same position as Fe in pure Pt (Fig. 3a). In the latter figure the bonding and antibonding interactions are below the Fermi level which indicates a totally repulsive interaction. In the former, owing to the influence of Fe, part of the antibonding interactions is above the Fermi level and the resulting interaction is attractive. This is also reflected in the DOS projected on d_{xz} (Fig. 2). The top of the Pt(1) d_{xz} band interacts with Fe d_{xz} which is higher in energy and is split into two components, one above the Fermi level and one farther below it. The rest of the band keeps the same shape. The fact that part of the band goes above the Fermi level is compensated by the increase of this level and hence the population of the orbitals does not vary much. The behavior of d_{z^2} and d_{yz} is explained in the same manner. Therefore, in contrast with the usual case, and by a compensation effect between DOS deformation and Fermi level shift, the orbitals that have the strongest interaction with the second layer Fe have the smallest change in their electronic occupation, while those with little interaction are populated by the Fermi level increase.

The effect of the Fe atoms is also transmitted to the surface Pt atoms of type 2 through Pt of type 1 and through the Pt atoms of the second layer (which we will call Pt of type 3). In fact, each type 3 Pt atom has three Fe as first neighbors, two in the same layer and one in the third layer. Therefore all its orbitals are modified like those of type 1 Pt, which means that their *d* bandwidth is slightly contracted and a small part is destabilized above the Fermi level. Figure 4 shows the change of d_{xz} Pt(2) and d_{yz} Pt(2) when Pt is alloyed with Fe. In the interactions between orbitals of Pt(2) and Pt(1) or Pt(3), part of the out-of-phase combinations lies above the Fermi level in the case of the $Pt_{80}Fe_{20}$ alloy compared to pure Pt. For example, the COOP curves between d_{yz} Pt(2) and d_{yz} Pt(3) are reproduced in Figs. 3c and 3d for the cases of pure Pt and of the alloy, respectively. The effect of Fe is not direct but of second order. Hence it is smaller for Pt(2) than for Pt(1) (compare, for example, d_{xz} Pt(1) and d_{xz} Pt(2) in $Pt_{80}Fe_{20}$ in Figs. 2 and 4) and the up-shift of the Fermi level induces a better electron gain for Pt(2). Therefore at the surface, the electron transfer from the more electropositive Fe atoms does not happen only toward their first neighbors because those are partly destabilized by the interaction, but is transmitted mainly to the farther Pt of type 2. This is a manifestation of the delocalized electronic structure and electron (or hole) reservoir effect at metallic surfaces.

The orbitals which stick out from the surface are those involved in the adsorption processes. Since their shape is considerably changed in the alloy, one can understand that alloying Pt with Fe will modify significantly the adsorption properties, even though the surface layer is still pure Pt. In the next sections we will compare the adsorption of various molecules (H, CO, C_2H_4, CH_2O) on both surfaces.

IV. ADSORPTION OF ATOMIC HYDROGEN ON Pt(111) AND $Pt_{80}Fe_{20}$(111)

The adsorption of atomic hydrogen on Pt(111) is well documented experimentally (11). It has been demonstrated that H is adsorbed in a hollow threefold site with a Pt–H distance of 1.9 Å. Hence we have considered only this adsorption site in the following. To our knowledge very few theoretical works deal with this subject (12) and they do not describe the interactions in terms of orbitals.

Two different threefold sites exist on a (111) surface of a fcc metal like Pt, namely one called fcc(1) with no atom in the second layer and one called hcp(2) with an atom in the second layer which is right below the 3-fold site. On the $Pt_{80}Fe_{20}$(111) surface (Scheme 1) there are four different threefold sites: (1) and (2) have a Pt atom below in the second or third layer as in the case of Pt(111). However, for $Pt_{80}Fe_{20}$, the atoms which are below the site in the second and third layers can be Fe atoms. This leads to two new sites: there is a hcp one (3) with a Fe atom just under it and a fcc one (4) with a Fe atom in the third layer.

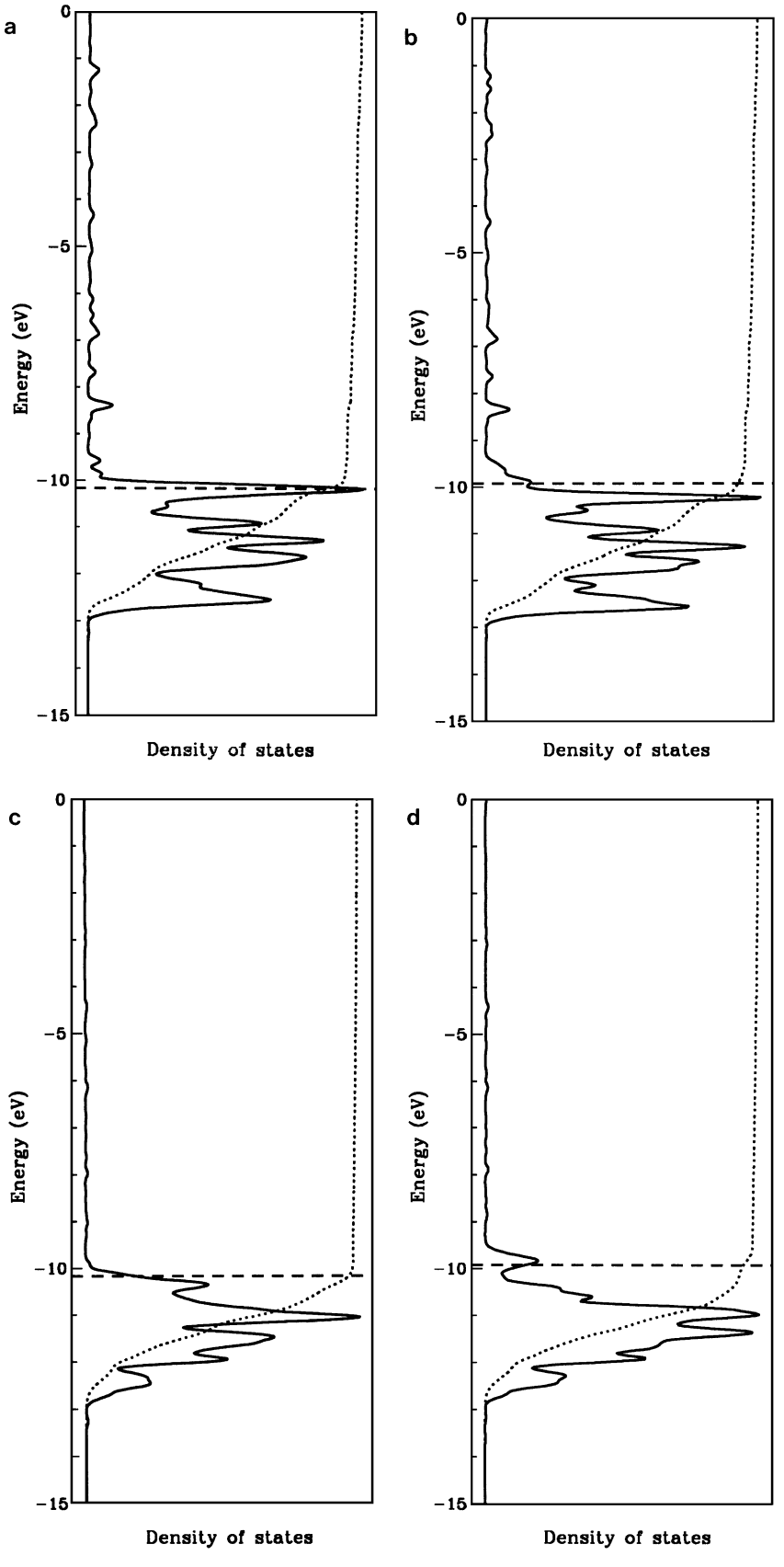

FIG. 2. Density of states (DOS) projected on d_{xy} Pt(1) (a) in Pt and (b) in $Pt_{80}Fe_{20}$ and DOS projected on d_{xz} Pt(1) (c) in Pt and (d) in $Pt_{80}Fe_{20}$.

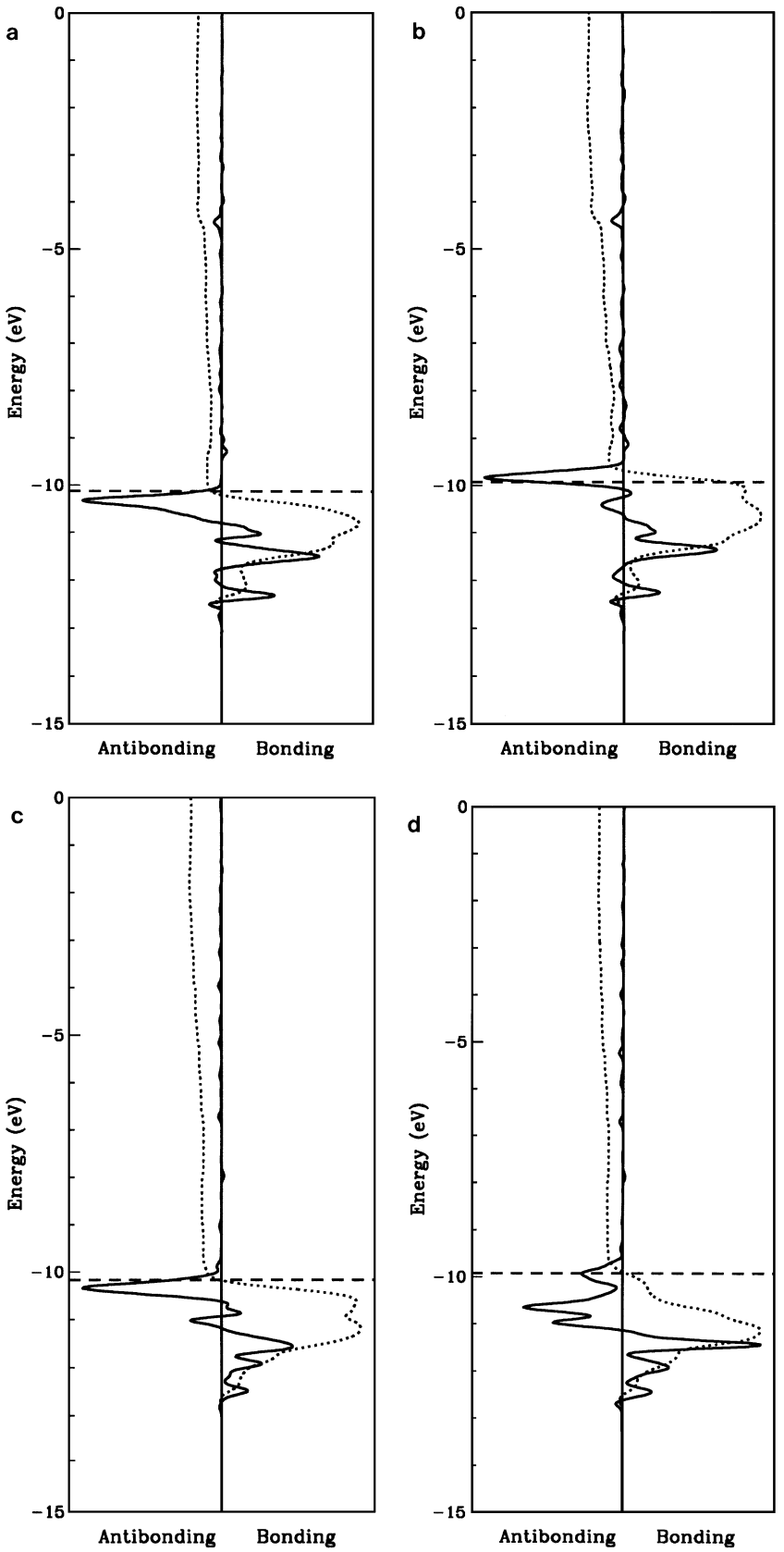

FIG. 3. Crystal orbital overlap population (COOP) between d_{xz} Pt(1) and (a) d_{xz} Pt(3) in Pt, (b) d_{xz} Fe in $Pt_{80}Fe_{20}$. COOP between d_{yz} Pt(2) and d_{yz} Pt(3) (c) in Pt, (d) in $Pt_{80}Fe_{20}$.

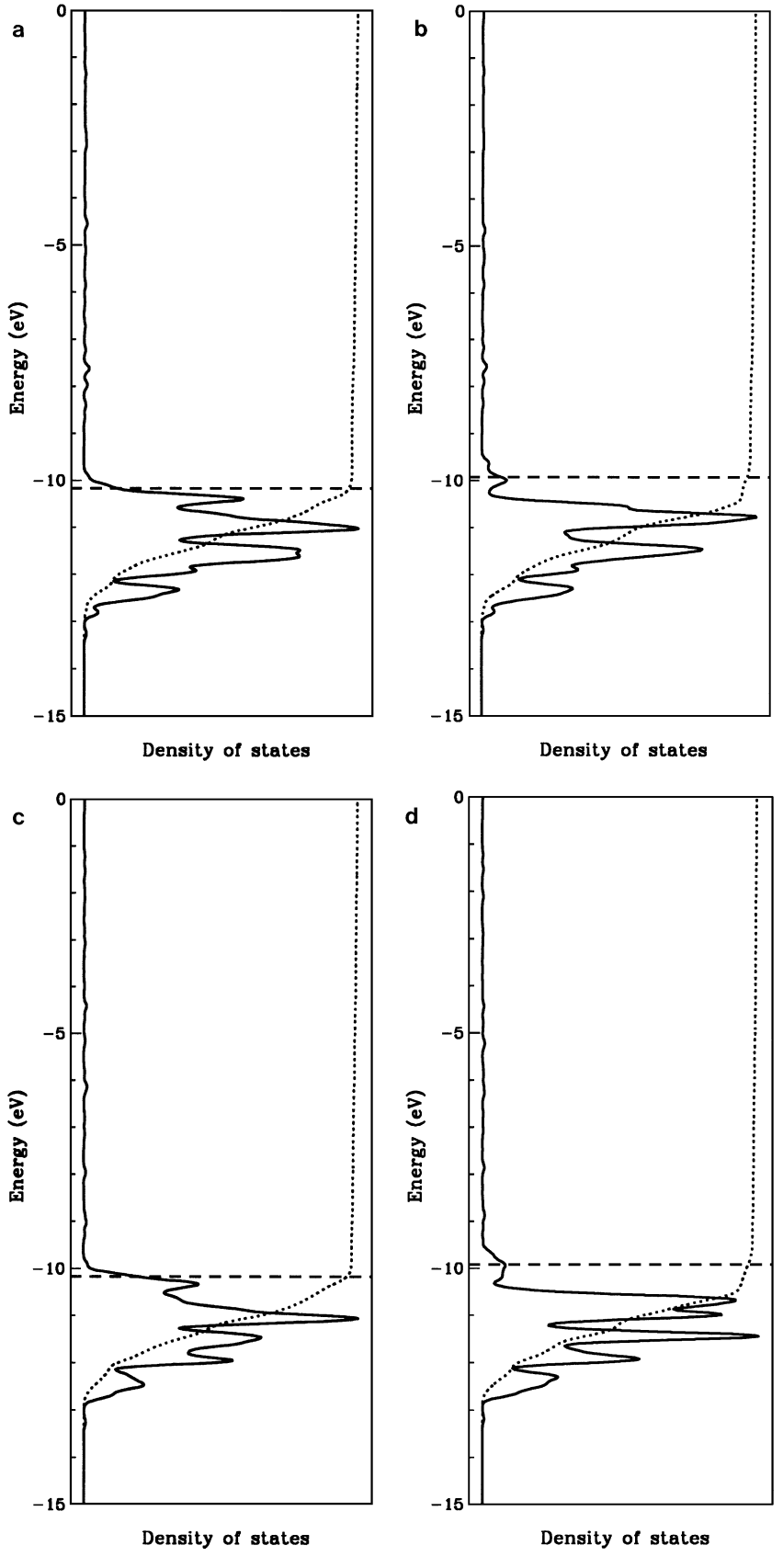

FIG. 4. Density of states (DOS) projected on d_{xz} Pt(2) (a) in Pt, (b) in $Pt_{80}Fe_{20}$. DOS projected on d_{yz} Pt(2) (c) in Pt, (d) in $Pt_{80}Fe_{20}$.

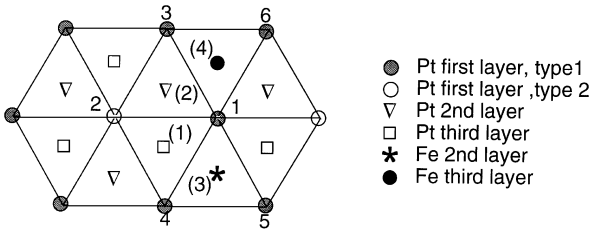

SCHEME 1

The adsorption of a hydrogen atom on these four sites has been studied with the two methods mentioned previously (band and cluster calculations). The binding energies (BE), given as the difference between the energy of the whole system and the energies of H and of the metallic part taken separately, are collected in Table 2. The more negative the value of BE, the more stable the adsorption. Let us make some comments on Table 2. First, both methods give almost the same binding energies. This is a justification of using a cluster to model a surface, if this cluster is large enough and if the edge effects are corrected. Second, on pure Pt, the fcc adsorption site is slightly more stable than the hcp one, in contradiction with some experimental results where the adsorption has been tentatively suggested to occur at the hcp site (11b, c). The small energy difference in the calculation does not allow one to draw a firm conclusion here.

On $Pt_{80}Fe_{20}$, these two sites are less stable than on Pt, in agreement with the experimental results (7) since the energy for desorption of the majority of the hydrogen is lower by at least 2 kcal/mol on the alloy than on Pt(111). However, on $Pt_{80}Fe_{20}$, the hcp(3) site with a Fe atom in the second layer competes with the fcc(1) site with the same binding energy. This means that the hcp site is more stable when the atom in the second layer is a Fe rather than a Pt atom. Following the stoichiometry of the second layer, there is one-quarter of Fe atoms and hence also one-quarter of hcp(3) sites. Experimentally, two peaks are present in the thermal desorption (TD) spectrum recorded on the alloy, in a ratio of roughly 1/4. Our calculation confirms that the second sort of adsorbed hydrogen corresponds to hollow sites with a Fe atom just below in the second layer.

TABLE 2

Binding Energies (in kcal/mol) for H Adsorption on the Hollow Sites of Pt(111) and $Pt_{80}Fe_{20}$(111) Surfaces

	Cluster		Band	
	Pt	$Pt_{80}Fe_{20}$	Pt	$Pt_{80}Fe_{20}$
fcc(1)	−77.1	−74.4(−72.5)	−76.3	−75.5(−72.6)
fcc(4)		−73.2(−70.4)		−72.7(−70.3)
hcp(2)	−75.5	−71.5(−68.9)	−74.6	−70.3(−68.1)
hcp(3)		−74.2(−73.5)		−75.7(−74.5)

Note: The values in parentheses correspond to $H_{ii} = -9.9$ eV for the *d* orbitals of iron instead of −10.5 eV.

A change in the H_{ii}'s of the Fe orbitals only slightly influences the results (see Table 2). If iron is taken more electropositive (H_{ii}'s $= -9.9$ eV), the phenomena are more pronounced. The hcp(3) site becomes more stable than the fcc(1) site which is in better quantitative agreement with the experiments. The interpretations based on the interactions between the molecular orbitals are made with these parameters because the effect is more clear-cut. In a threefold site, all metal orbitals except d_{z^2} are involved in the interaction with the *s* H orbital. Orbitals p_x and p_y, $d_{x^2-y^2}$ and d_{xy}, d_{xz} and d_{yz} are combined or not depending on the atom considered. The interaction with d_{z^2} is nonbonding. The fact that p_x, p_y, $d_{x^2-y^2}$, and d_{xy} are involved in the interaction is due to the short distance of H from the surface (1 Å). In Table 3 are given the overlap populations between *s* H and the atomic orbitals of each metal atom and the total overlap populations between H and the three metal atoms. Atom 1 belonging to all adsorption sites is not considered. In all cases the interactions between *s*, p_x, p_y, and p_z Pt and *s* H are improved on PtFe compared to pure Pt and the interactions of the *d* orbitals are in contrast weakened. The result is that globally the stabilizing interactions are smaller on the alloy than on Pt which is reflected by a decrease in the total overlap population between H and the three metal atoms.

The interactions between the *s* H orbital and the orbitals of the metals are of the same classical type as those described previously (8, 13). Such interactions push a part of the *d* band above the Fermi level, which results in a loss of electrons from the *d* band. In contrast, part of the *s–p* band is pulled below this level and hence gains some electrons. This is effectively the case although the transfers are small (from 0.02 to 0.08 e^-). The DOS projected on d_{yz} Pt_4 before and after H adsorption (Fig. 5) show that the *s* H orbital has been strongly stabilized relative to its atomic position (−12.1 eV) and that the *d* band has been partly pushed above E_F. The larger the part of the *d* band pushed above E_F, the less destabilizing the interaction. We have seen before that the effect of alloying Pt with Fe is to shift up the Fermi level and to reduce slightly the *d* bandwidth. Therefore compared to pure Pt the *d* band is farther from and the *s* band is closer to E_F in the alloy. The consequence is that a smaller part of the *d* band can be pushed above E_F and, in contrast, a larger part of the *sp* band can be pushed below E_F for the PtFe alloy, which explains the results obtained (Table 3). We have also seen that the effect of the presence of Fe atoms is more pronounced for Pt atoms of type 2 (numbered Pt_2 in Scheme 1) than for Pt atoms of type 1 like Pt_4 or Pt_5. The result is a larger decrease of the H interactions with Pt_2 than with Pt_3 or Pt_4 reflected by smaller overlap populations with Pt_2. Therefore the hollow

TABLE 3

Bonding Characteristics of the Hollow Adsorption Modes of Hydrogen on Pt(111) and $Pt_{80}Fe_{20}(111)$

		Pt	$Pt_{80}Fe_{20}$		
		fcc(1)	fcc(1)	hcp(2)	hcp(3)
BE(kcal/mol)		−77.1	−72.5	−68.9	−73.5
Charge on H		−0.18	−0.22	−0.23	−0.22
Overlap population (op) between *s* H and Pt_2	*s*	0.108	0.108	0.110	
	p_x	0.022	0.026	0.028	
	p_y	0.007	0.009	0.009	
	p_z	0.022	0.025	0.027	
	$d_{x^2-y^2}$	0.004	0.002	0.002	
	d_{z^2}	−0.001	−0.001	−0.001	
	d_{xy}	0.012	0.007	0.007	
	d_{xz}	0.028	0.020	0.019	
	d_{yz}	0.009	0.007	0.007	
Pt_3 or Pt_4 or Pt_5	*s*	0.108	0.113	0.107	0.112
	p_x	0	0	0	0.026
	p_y	0.029	0.035	0.037	0.009
	p_z	0.022	0.026	0.029	0.026
	$d_{x^2-y^2}$	0.016	0.011	0.007	0.002
	d_{z^2}	−0.001	−0.001	−0.001	−0.001
	d_{xy}	0	0	0	0.006
	d_{xz}	0	0	0	0.024
	d_{yz}	0.037	0.031	0.027	0.008
Total op between H and Pt[a]		0.638	0.634	0.631	0.634
op Pt–Pt		0.093(0.143)[b]	0.085(0.141)	0.088(0.144)	0.091(0.152)

[a] Overlap population between Pt_1 and H has been added to obtain total op.
[b] In parentheses are given the Pt–Pt overlap populations on the bare cluster.

sites containing a Pt atom of type 2 are less favored than those containing Pt atoms of type 1.

Let us see now why the hcp(3) site is the most stable. First, it contains no atom of type 2. Second, there exists a stabilizing interaction between H and the Fe atom in the second layer as indicated by the overlap population of 0.002 between *s* H and d_{z^2} Fe. Nevertheless, this interaction is very small and the stability is mainly due to the fact that hcp(3) is only surrounded by Pt of type 1.

V. ADSORPTION OF CO ON Pt(111) AND $Pt_{80}Fe_{20}(111)$

The adsorption of CO on Pt(111) has also been extensively studied (14). The molecule is adsorbed perpendicular to the surface on a top site at low coverage and on a bridge site at higher coverage. The metal–carbon bond lengths have been determined by LEED for both sites (15): these are 1.85 Å for the on-top site and 2.08 Å for the bridge site with a C–O bond length of 1.15 Å. These values are used in this work. A few theoretical works also exist on this subject, both on clusters (16) and on surfaces (17). In order to compare the adsorption of CO on pure Pt and on the alloy, we have been obliged to reconsider the former.

As for H adsorption, both methods have been used, the cluster and the periodic surface. Only the on-top and the bridge adsorption sites have been considered, the hollow site being less stable according to the calculations and not detected experimentally with certainty.

On the $Pt_{80}Fe_{20}(111)$ surface there are two on-top sites a and b (one on each Pt type) and three different bridge sites, one between Pt atoms of type 1 with a Pt in the second layer (bridge c), one between Pt atoms of type 1 with a Fe in the second layer (bridge d), and one between one Pt of type 1 and one Pt of type 2 (bridge e) (see Scheme 2 for the notations). The binding energies obtained with the two methods mentioned above are given in Table 4. As for H adsorption, both methods give similar results. As previously described (14), the bridge site on Pt(111) is less

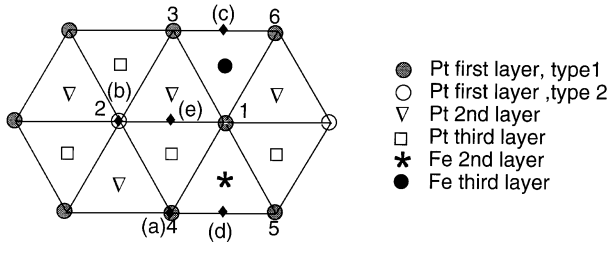

SCHEME 2

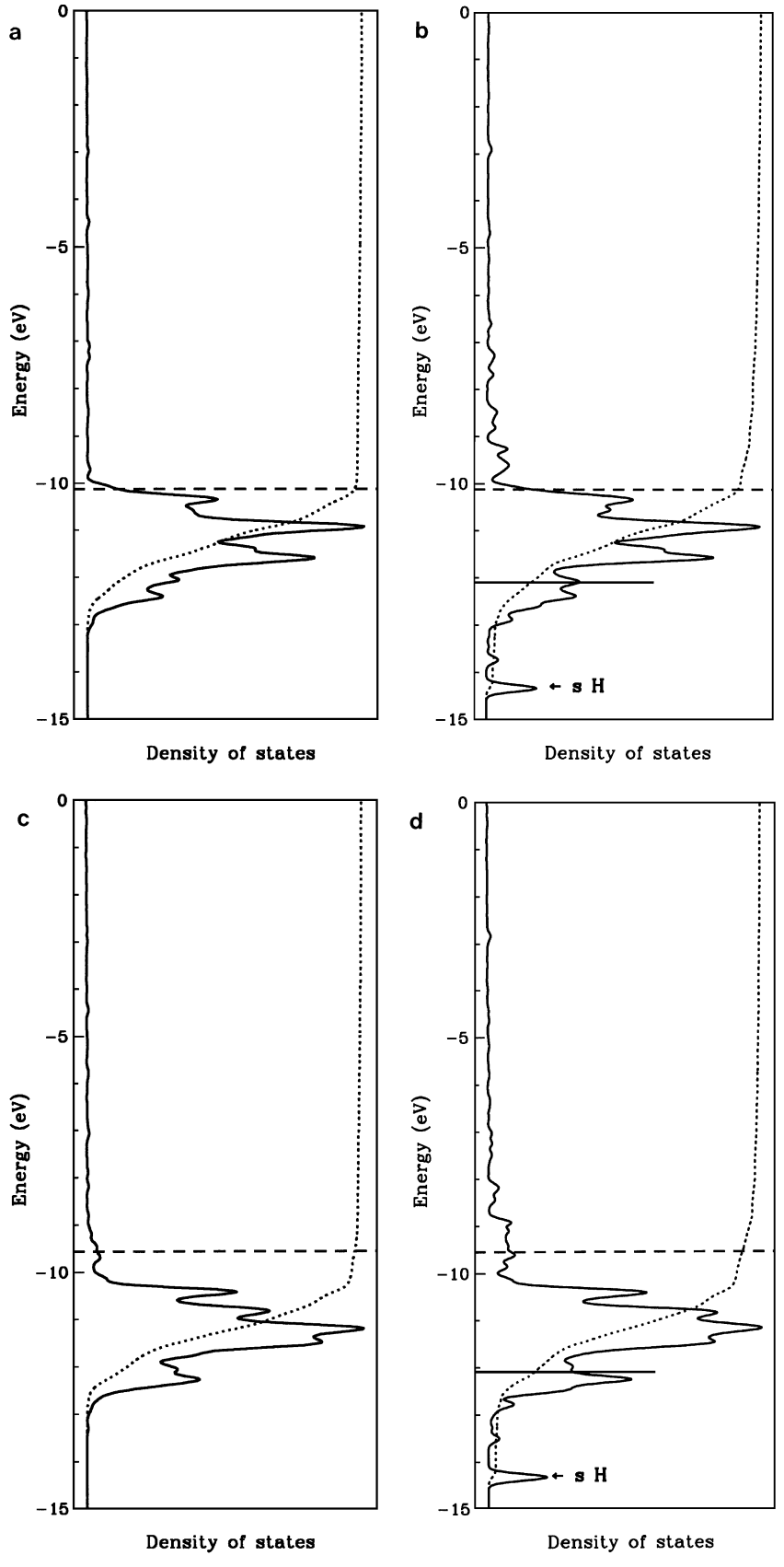

FIG. 5. Density of states (DOS) projected on d_{yz} Pt_4 (see numbering on Scheme 1) before and after H adsorption in the fcc(1) site: (a), (b) on Pt; (c), (d) on $Pt_{80}Fe_{20}$. The H_{ii} value used for Fe is −9.9 eV (E_F is higher than in previous Figures). In (b) and (d) the horizontal line represents the position of *s* H in the free atom.

TABLE 4

Binding Energies (in kcal/mol) for CO Adsorption on Pt(111) and $Pt_{80}Fe_{20}$(111) Surfaces

	Cluster		Band	
	Pt	$Pt_{80}Fe_{20}$	Pt	$Pt_{80}Fe_{20}$
on-top a	−68.9	−61.1(−53.1)	−68.5	−62.6(−52.8)
on-top b		−60.5(−51.1)		−60.7(−49.5)
bridge c	−66.5	−58.0(−49.6)	−66.0	−58.1(−50.1)
bridge d		−60.5(−52.9)		−62.4(−53.4)
bridge e		−58.3(−49.6)		−57.4(−48.0)

Note: The values in parentheses correspond to $H_{ii} = -9.9$ eV for the *d* orbitals of ion instead of −10.5 eV.

stable than the on-top one explaining why on-top sites are populated first. On $Pt_{80}Fe_{20}$(111) the main feature is that the bridge site d becomes as stable as the on-top site a or even more stable depending on the method and on the H_{ii}'s value of the Fe *d* orbitals. In contrast, the on-top site b which is on a Pt of type 2 remains less stable whatever the method. Furthermore, when compared with Pt(111), all binding energies are smaller on $Pt_{80}Fe_{20}$(111). What happens experimentally? Two peaks appear in the CO TD spectrum from $Pt_{80}Fe_{20}$(111) in the ratio 1/4 (6). The activation energy for desorption for the main peak is lower than on the Pt(111) surface, in agreement with our results. The electron energy loss (HREEL) spectrum of adsorbed CO on $Pt_{80}Fe_{20}$(111) shows two peaks at 2100 and 1860 cm^{-1} which correspond to CO adsorbed on-top and bridged, respectively. The 1860 cm^{-1} peak exists even at low coverage (0.06 L) whereas on Pt(111) it appears only at higher coverage (0.4 L) (14a), which would mean that a bridge site coexists with the on-top site on $Pt_{80}Fe_{20}$(111) even at low coverage, in contrast to the situation on Pt(111). Our calculations confirm this hypothesis since we find one bridge site to be as stable as the on-top site. Moreover, this bridge site having a Fe atom just below is as numerous as the Fe atoms in the second layer, that is in a ratio 1/4 relative to the on-top site which is on Pt of type 1. Therefore the two sites we find the most stable are in the same ratio as the peaks in the TD spectrum. Hence our conclusion would be that the two forms that exist on $Pt_{80}Fe_{20}$(111) are one on-top and one bridged forms and not two on-top forms on the two kinds of Pt atoms, as has been suggested (7).

Let us now interpret these results. The interaction of CO with a surface has already been well described (17). The 4σ and 5σ orbitals of CO donate electrons to the metal and, by back-donation, the π^* orbitals which are C–O antibonding receive electrons. Our results are given in Table 5. For the bridge site on Pt(111), donation from the occupied bonding orbitals 4σ and 5σ is weakly modified compared to the on-top site while back-bonding toward the antibonding π^* orbitals (especially π_y^*) is significantly increased. These two electron movements contribute to weaken the C–O bond (the CO overlap population is 1.140 and 1.187 for the bridge and the on-top, respectively). Since more orbitals are involved in the bridge geometry, the total electron transfer is better and so is the Pt–C overlap population. Hence, why is it less stable?

In our previous works (8) we have pointed out the important role of the four-electron destabilizing interactions. They were quantified by the square of the overlaps S^2 between the occupied orbitals of the adsorbed molecule and the filled states of the metal. By doing that, the repulsions can be slightly overestimated since we have seen that the filled *d* bands can be partly emptied by interaction with the adsorbate and so can participate in the attractive interactions. We have therefore modified our calculation of S^2 by only taking into account the pairs of orbitals for which the sum of electron occupations in the interacting system is greater than 3 and by weighting each S^2 term by the electron excess beyond 3. The corrected S^2 values for CO adsorption are given in Table 5. We have already observed that the more numerous the atoms involved in the adsorption, the larger the S^2 term. Effectively, in the present case, the repulsive S^2 term is larger for the bridge site than for the on-top site. The better bonding of CO on the bridge site is balanced by a weakening of the C–O bond and of the metal–metal bonds and by a larger repulsive term. Hence the bridge site is less stable than the on-top one.

Let us compare these results with those obtained for $Pt_{80}Fe_{20}$(111). For each type of site, the donation from 4σ and 5σ orbitals is slightly smaller on the alloy and, in contrast, the back-donation to π_x^* and π_y^* is slightly larger or equal. The differences are very small and balance each other so that the total electron transfer and the C–O and Pt–C overlap populations are nearly the same for the alloy and for pure Pt. This explains why experimentally the EELS

TABLE 5

Bonding Characteristics of the Adsorption Modes of CO on Pt(111) and $Pt_{80}Fe_{20}$(111)

	Pt		$Pt_{80}Fe_{20}$			
	top	bridge	top a	top b	bridge d	bridge e
BE(kcal/mol)	−68.9	−66.5	−61.1	−60.5	−60.5	−58.3
op C–O	1.187	1.140	1.187	1.188	1.139	1.140
op Pt–C(total)	0.816	0.886	0.815	0.815	0.886	0.885
op Pt–Pt	0.135	0.072	0.129	0.129	0.063	0.065
Loss of 4σ	0.20	0.20	0.19	0.19	0.20	0.20
Loss of 5σ	0.43	0.46	0.41	0.43	0.45	0.45
Gain of π_x^*	0.18	0.20	0.18	0.18	0.21	0.18
Gain of π_y^*	0.18	0.34	0.19	0.18	0.34	0.36
Charge on CO	0.26	0.13	0.24	0.26	0.11	0.12
Total electron transfer	0.99	1.20	0.97	0.98	1.20	1.20
$S^2 \times 10^{-2}$	9.98	13.26	10.45	10.78	14.12	14.04

vibrational frequencies for CO are not changed between Pt(111) and $Pt_{80}Fe_{20}$(111). The variations in the electron transfers are explained as in the case of H adsorption. The interactions of the occupied 4σ and 5σ orbitals with the almost-filled *d* orbitals of the metal are all the more destabilizing as a smaller part of these *d* orbitals is pushed above the Fermi level, as it occurs on the alloy. In contrast, the vacant π^* orbitals have the more easily a bonding part below the Fermi level as this level is higher, which is the case for the alloy.

An important feature is that the repulsive term is larger on the alloy than on pure Pt metal. Since the *d* bands of Pt atoms in the alloy are farther below the Fermi level compared to pure platinum, there are more occupied states taking part in the repulsive term. This corresponds to the small electronic population excess of Pt in the alloy. Moreover, these *d* bands are less pushed above the Fermi level by the interactions with the adsorbate and hence a larger part of them is involved in the calculation of S^2. Therefore, the principal cause of the smaller binding energies on the alloy rests on the larger repulsive term and not on a change in the electron transfer. For the bridge sites near a Pt atom in the second layer (like bridge c or bridge e), a small negative overlap population exists between C and this Pt atom. This overlap population becomes quasi-nil when a Fe is in the second layer. This can explain why bridge d is the most stable of the bridge sites.

VI. ADSORPTION OF ETHYLENE, FORMALDEHYDE, ACROLEIN, AND CROTONALDEHYDE ON Pt(111) AND $Pt_{80}Fe_{20}$(111)

VI.1. Adsorption of Ethylene and Formaldehyde

The adsorption of these molecules on Pt(111) has already been studied by us (8). In all cases, the best adsorption geometry is the di-σ one where the molecules lie parallel to the surface with two metal atoms involved in the interaction (see Scheme 3). In order to avoid hindrance between the adsorbed molecules, we have chosen the cluster method where only one molecule is adsorbed.

According to Scheme 2, three possibilities exist for the di-σ mode, i.e., di-σ_{4-5}, di-σ_{2-3}, and di-σ_{3-6}, depending on the two Pt atoms involved. Let us first consider ethylene (Table 6). On $Pt_{80}Fe_{20}$(111), the three di-σ geometries are close in energy, with di-σ_{4-5} slightly more stable. They all are less stable than the di-σ mode on pure Pt by 7–8 kcal/mol. The total electron transfer is smaller on the alloy. This is due to a decrease of the π donation into the cluster not being balanced by a very small increase of the π^* back-donation. This behavior is the same as that described for H and CO adsorptions and the explanations are identical: compared to pure Pt, the electron donations into the alloy are decreased and the back-donation to the molecule is increased. Similarly to CO adsorption also, the repulsive term (S^2) is greater on the alloy, which, combined with a smaller electron transfer, explains the decrease in the binding energies.

Formaldehyde (CH_2O) behaves similarly except that the increase in the π^* backdonation is larger than the decrease in the π donation, which results globally in a better total transfer on the alloy than on pure Pt. We have already pointed out that the π^* orbital plays a more important role for the adsorption of a C=O bond than of a C=C bond, owing to its lower energy position. Hence the variation of the electron transfer and of S^2 are of opposite influence which explains that the decrease in binding energy is smaller than for ethylene. It must be added that there are two possible orientations for the di-σ_{2-3} geometry, one where the oxygen atom is bound to Pt_2 (type 2) and the other where O is bound to Pt_3 (type 1). The better one is the latter (by 2 kcal/mol). This is due to a larger S^2 term in the former.

VI.2. Adsorption of Acrolein and Crotonaldehyde

Acrolein comprises both C=C and C=O double bonds as previously described. On Pt(111), the molecule is preferentially adsorbed through the C=C bond (di-σ_{CC}) with a secondary interaction involving the oxygen atom, giving a kind of trihapto η_3 mode (Scheme 4) (8d). The simple di-σ_{CC} η_2 geometry and the di-σ_{CO} geometry are 2.2 and 3.5 kcal/mol, respectively, less stable than the η_3 one (Table 7).

The same three adsorption modes have been calculated on $Pt_{80}Fe_{20}$(111). As for ethylene and formaldehyde, the binding energy is reduced on $Pt_{80}Fe_{20}$(111) compared to Pt(111) for both double bonds and more for the C=C bond than for the C=O bond. In contrast to the situation existing on pure Pt, the best di-σ_{CC} form in the alloy is the η_2 form where no interaction occurs between the oxygen and the

di-σ_{CC} di-σ_{CO}

SCHEME 3

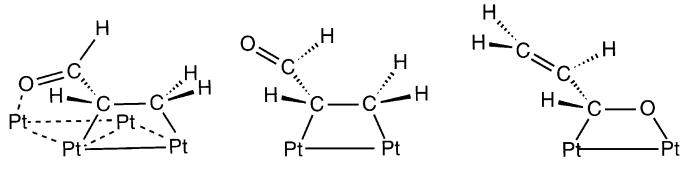

di-σ_{CC} η_3 di-σ_{CC} η_2 di-σ_{CO} η_2

SCHEME 4

TABLE 6

Bonding Characteristics of the di-σ Adsorption Modes of Ethylene (di-σ_{CC}) and Formaldehyde (di-σ_{CO}) on Pt(111) and $Pt_{80}Fe_{20}$(111)

		$Pt_{80}Fe_{20}$		
	Pt	4–5[a]	2–3	3–6
		C_2H_4		
BE(kcal/mol)	−14.8	−7.6	−6.4	−6.1
op C–C	0.824(1.287)[b]	0.827	0.826	0.835
op Pt–C (total)	0.826	0.828	0.830	0.830
op Pt–Pt	0.114(0.144)	0.107(0.142)	0.108(0.143)	0.111(0.140)
Electron transfer				
π	0.72	0.69	0.70	0.63
π^*	0.63	0.63	0.64	0.64
Total	1.45	1.43	1.44	1.38
$S^2 \times 10^{-2}$	11.21	11.97	11.98	11.76
		CH_2O		
BE(kcal/mol)	−19.8	−15.4	−15.5	−15.0
op C–O	0.559(0.930)	0.554	0.556	0.557
op Pt–C	0.444	0.450	0.449	0.449
op Pt–O	0.293	0.282	0.277	0.277
op Pt–Pt	0.110	0.100	0.100	0.103
Electron transfer				
π	0.24	0.23	0.22	0.22
π^*	0.91	0.94	0.92	0.95
Total	1.27	1.29	1.26	1.28
$S^2 \times 10^{-2}$	10.05	10.68	10.69	10.16

[a] This numbering is taken from Scheme 2.
[b] The values in parentheses correspond to the bare cluster or to the free molecule.

surface. The strength of this interaction can be evaluated by suppressing the overlap between the oxygen and the surface. One obtains a loss of 5 kcal/mol on Pt(111) and only 1 kcal/mol on $Pt_{80}Fe_{20}$(111). Therefore the interaction of O with the surface is more stabilizing on pure Pt than on the alloy. This is due to a smaller electron transfer from O to Pt (0.16 instead of 0.19) together with a larger repulsive term since all repulsive interactions are enhanced on the alloy. In conclusion, the interaction of O with the surface on the alloy is not strong enough to balance the deformation energy

TABLE 7

Bonding Characteristics of the Various Adsorption Modes of Acrolein and Crotonaldehyde on Pt(111) and $Pt_{80}Fe_{20}$(111)

	Pt			$Pt_{80}Fe_{20}$					
	di-σ_{CC}		di-σ_{CO}	di-σ_{CC}(4–5)[a]		di-σ_{CC}(2–3)		di-σ_{CO} 4–5	di-σ_{CO} 2–3
	η_3[b]	η_2[b]		η_3	η_2	η_3	η_2		
				CH_2=CH–CHO					
BE(kcal/mol)	−17.1	−14.9	−13.6	−5.4	−8.1	−5.1	−7.1	−8.7	−8.6
Electron transfer									
π	0.75	0.64	0.18	0.71	0.62	0.72	0.60	0.17	0.16
π^*	0.53	0.69	0.80	0.54	0.71	0.54	0.71	0.83	0.83
p_O	0.19			0.16		0.16			
Total	1.75	1.47	1.26	1.68	1.46	1.70	1.44	1.27	1.26
$S^2 \times 10^{-2}$	16.8	12.4	11.9	17.9	13.2	17.7	13.3	12.7	12.7
				CH_3CH=CH–CHO					
BE(kcal/mol)	−10.7		−11.3		−0.6			−6.2	

[a] This numbering is taken from Scheme 2.
[b] Taken from Scheme 4.

needed to break the conjugation of the two double bonds and to allow O to approach the surface. It must be added that, in the case of the di-$\sigma_{CC(4-5)}$ form, two possibilities exist for the additional oxygen interaction: either O interacts with a Pt of type 1 or with a Pt of type 2. The former interaction is preferred by 2.8 kcal/mol, essentially because the repulsive term is smaller on a Pt of type 1 and only this geometry has been considered.

Three interesting conclusions can be drawn from these results. First, the di-σ_{CC} adsorption mode of acrolein is not the same on Pt(111) and on $Pt_{80}Fe_{20}$(111). They differ by the direct oxygen interaction with the surface (present on Pt(111) and absent on the alloy). Second, acrolein is less strongly adsorbed on the alloy, and third the di-σ_{CO} adsorption geometry becomes the best one, contrary to the situation on pure Pt. Since the difference between the binding energies is small (0.6 kcal/mol) one can say that the di-σ_{CC} and the di-σ_{CO} modes are equally allowed.

The same calculations made on crotonaldehyde (2-methyl propenal) lead to the same results. This aldehyde, which is adsorbed roughly equally through both double bonds on Pt(111), strongly prefers the di-σ_{CO} form on the alloy. Therefore, the general trends for adsorption of α–β ethylenic aldehydes are as follows: the molecules are less strongly adsorbed and they have a more pronounced tendency to adsorb through the C=O bond on the alloy than on pure Pt.

These conclusions can explain the experimental results. Effectively, it has been shown that $Pt_{80}Fe_{20}$(111) has a higher activity for the hydrogenation of crotonaldehyde and methyl crotonaldehyde and a better selectivity in unsaturated alcohol compared to Pt(111) (2). The same trends have been observed for the hydrogenation of cinnamaldehyde on crystallites of Pt–Fe alloys supported on charcoal (1). If one assumes that the hydrogenated bond is the adsorbed one, our results explain why the formation of the unsaturated alcohol, by hydrogenation of the C=O bond, is more preferred on the alloy than on pure platinum. The higher reactivity is more difficult to explain because it would require reaction path and barrier determination. However, this increased reactivity can be related to the weakest chemisorption on PtFe of both reactants, unsaturated aldehyde and hydrogen (see Section IV).

VII. CONCLUSION

The extended Hückel calculations performed in this work allow an understanding of the behavior of the $Pt_{80}Fe_{20}$(111) surface alloy and especially they support the conclusion that the modifications of the catalytic properties when Pt is alloyed with Fe come from modifications of the electronic structure of the surface Pt atoms.

First, even though the surface plane is all Pt, two kinds of Pt atoms are present, which have different behavior concerning the adsorption of molecules. Compared to surface atoms of pure Pt(111), the surface atoms of $Pt_{80}Fe_{20}$(111) are more negatively charged because of a charge transfer from Fe to Pt. Surprisingly, the atoms that are the most modified are those of type 2 that have no Fe as neighbor. The Fermi level is higher in the alloy and the DOS projected on the orbitals pointing out of the surface (d_{z^2}, d_{xz}, d_{yz}) are narrower.

As regards chemisorption, all the species which have been studied are less strongly adsorbed on the alloy than on the pure metal, which can explain the enhancement in catalytic activity of the alloy if one invokes the volcano-curve concept (18). Generally speaking, the electron donation from the molecule to the surface is decreased on the alloy relative to the pure metal. On the contrary, the back-donation from the surface to the molecule is increased. These variations are small and the total electron transfer depends on their balance, resulting either in a slightly smaller transfer (CO, C_2H_4) or in a slightly greater transfer (CH_2O). The principal feature is the larger repulsive term for the alloy which is the main cause of the decrease of the binding energies. The repulsions increase for two reasons. First, some orbitals ($d_{x^2-y^2}$, d_{xy}) lose their peak above the Fermi level and become entirely below this level on the alloy (see Fig. 2), which means that more levels are doubly occupied and give rise to repulsion. Second, the other orbitals (d_{z^2}, d_{xz}, d_{yz}) which interact with the adsorbates have their main part farther from the Fermi level on the alloy than on pure metal. Hence a smaller part can be pushed above the Fermi level by the interactions with the adsorbates and this results also in a larger repulsive term. Therefore, the increase of repulsions on the alloy is principally due to the raising up of the Fermi level resulting in an increased electron density on the surface Pt atoms.

On $Pt_{80}Fe_{20}$(111), two adsorption sites exist for each molecule, but with a very small energy difference (ca. 1 kcal/mol). The first is the same as on Pt(111); the second is due to the presence of Fe atoms in the second layer. For hydrogen, the new adsorption site is a hollow hcp with a Fe atom in the second layer. For CO it is a bridge site close also to a Fe atom rather than an on-top site, as has been postulated experimentally (6). For ethylene also, two sites can be distinguished. For formaldehyde, in contrast, they are identical.

One of the most interesting results is the trend manifested by the α–β unsaturated aldehydes to change their adsorption mode when Pt is alloyed with Fe: the di-σ_{CO} adsorption mode becomes predominant over the di-σ_{CC} one. These important changes in the adsorption modes explain why the catalytic behavior of pure Pt and PtFe alloy are so different in regard to the selectivity of the hydrogenation reactions. For example, our results explain the better selectivity in unsaturated alcohol on the $Pt_{80}Fe_{20}$ alloy.

The qualitative arguments extracted from these calculations go beyond the strict example of the $Pt_{80}Fe_{20}(111)$ alloy. They indicate that the small perturbation (small charge transfer) induced by alloying can have a large influence on the surface reactivity, for example by changing the chimisorption mode of the adsorbate, and this even when the alloying element is not present at the surface site. Another general implication is that alloying a Group 10 metal with a more electropositive element results in a small population excess on the former metal, which generally increases the four-electron repulsions, and hence yields less stable adsorptions. This effect can be responsible for an increased activity often observed with such alloys.

APPENDIX

For the periodic calculations, the tight-binding extended Hückel method, with a weighted H_{ij} approximation, has been applied (19). A three-layer slab has been used. However, we have verified for H adsorption that the stability order of the various sites is not modified with a four-layer slab and a seven-layer slab. The number of K points was 15 but the same energy values are obtained with 28 K points.

Platinum being a metal of the third row in the periodic table, the influence of the spin–orbit coupling can be important. Hence we have tested this effect for the adsorption of H and CO, both on Pt(111) and $Pt_{80}Fe_{20}(111)$ by introducing spin–orbit coupling in the program of band calculations (20). The parameter ξ of spin–orbit coupling was 0.62 eV (atomic value). A splitting of the *d* band is observed as expected and the Fermi level is raised by 0.3 eV for Pt(111) and by 0.07 eV for $Pt_{80}Fe_{20}(111)$. The binding energies for H and CO adsorptions are all increased when spin–orbit coupling is introduced but the relative order of the different sites is not changed. The adsorbed molecules are more negatively charged, which means that the electron transfer from the surface to the adsorbate is increased. Nevertheless, the conclusion is that spin–orbit coupling does not fundamentally change the results.

REFERENCES

1. (a) Goupil, D., Fouilloux, P., and Maurel, R., *Reaction Kinet. Catal. Lett.* **35**, 185 (1987); (b) Richard, D., Fouilloux, P., and Gallezot, P., "Proceedings, 9th International Congress on Catalysis, Calgary, 1988" (M. J. Phillips and M. Ternan, Eds), Vol. 3, p. 1074. Chem. Inst. of Canada, Ottawa, 1988.
2. Beccat, P., Bertolini, J. C., Gauthier, Y., Massardier, J., and Ruiz, P., *J. Catal.* **126**, 451 (1990).
3. Bertolini, J. C., and Massardier, J., *Catal. Lett.* **9**, 183 (1991).
4. Beccat, P., Gauthier, Y., Baudoing-Savois, R., and Bertolini, J. C., *Surf. Sci.* **238**, 105 (1990).
5. Barrett, N., Guillot, C., Bertolini, J. C., Massardier, J., and Khanra, B. C., *Surf. Sci. Lett.* **260**, L11 (1992).
6. Atli, A., Abon, M., Beccat, P., Bertolini, J. C., and Tardy, B., *Surf. Sci.* **302**, 121 (1994).
7. Atli, A., Alnot, M., Ehrhardt, J. J., Bertolini, J. C., and Abon, M., *Surf. Sci.* **269/270**, 365 (1992).
8. (a) Sautet, P., and Paul, J. F., *Catal. Lett.* **9**, 245 (1991); (b) Delbecq, F., and Sautet, P., *Catal. Lett.* **28**, 89 (1994); (c) Delbecq, F., and Sautet, P., *Langmuir* **9**, 197 (1993) and *Surf. Sci.* **295**, 353 (1993); (d) Delbecq, F., and Sautet, P., *J. Catal.* **152**, 217 (1995).
9. Hlil, E. K., Baudoing-Savois, R., Moraweck, B., and Renouprez, A. J., *J. Phys. Chem.* **100**, 3102 (1996).
10. Saillard, J. Y., and Hoffmann, R., *J. Am. Chem. Soc.* **106**, 2006 (1984).
11. (a) Sayers, C. M., *Surf. Sci.* **143**, 411 (1984); (b) Batra, I. P., *Surf. Sci.* **137**, L97 (1984); (c) Batra, I. P., Barker, J. A., and Averbach, D. J., *J. Vac. Sci. Technol. A* **2**, 943 (1984); (d) Christmann, K. R., *in* "Hydrogen Effects in Catalysis Fundamentals and Practical Applications" (Z. Paál and P. G. Menon, Eds). Dekker, New York, 1988.
12. (a) Tantardini, G. F., and Simonetta, M., *Surf. Sci.* **105**, 517 (1981); (b) Christensen, O. B., Stoltze, P., Jacobsen, K. W., and Nørskov, J. K., *Phys. Rev. B* **41**, 12413 (1990).
13. Hoffmann, R., *Rev. Mod. Phys.* **60**, 601 (1988).
14. (a) Hopster, H., and Ibach, H., *Surf. Sci.* **77**, 109 (1978); (b) Steininger, H., Lehwald, S., and Ibach, H., *Surf. Sci.* **123**, 264 (1982).
15. Ogletree, D. F., van Hove, M. A., and Somorjai, G. A., *Surf. Sci.* **173**, 351 (1986).
16. (a) Ray, N. K., and Anderson, A. B., *Surf. Sci.* **119**, 35 (1982); (b) Gavezzoti, A., Tantardini, G. F., and Miessner, H., *J. Phys. Chem.* **92**, 872 (1988).
17. Yat-Ting Wong and Hoffmann, R., *J. Phys. Chem.* **95**, 859 (1991).
18. Boitiaux, J. P., Cosyns, J., and Robert, R., *Appl. Catal.* **32**, 145 (1987).
19. Whangbo, M. H., and Hoffmann, R., *J. Am. Chem. Soc.* **100**, 6093 (1978).
20. Moraweck, B., unpublished work.